



**HAL**  
open science

## Pathogenesis of Hepatic Tumors following Gene Therapy in Murine and Canine Models of Glycogen Storage Disease

Hye-Ri Kang, Monika Gjorgjieva, Stephanie Smith, Elizabeth Brooks, Zelin Chen, Shawn Burgess, Randy Chandler, Lauren Waskowicz, Kylie Grady, Songtao Li, et al.

### ► To cite this version:

Hye-Ri Kang, Monika Gjorgjieva, Stephanie Smith, Elizabeth Brooks, Zelin Chen, et al.. Pathogenesis of Hepatic Tumors following Gene Therapy in Murine and Canine Models of Glycogen Storage Disease. *Molecular Therapy - Methods and Clinical Development*, 2019, 15, pp.383-391. 10.1016/j.omtm.2019.10.016 . inserm-02490225

**HAL Id: inserm-02490225**

**<https://inserm.hal.science/inserm-02490225>**

Submitted on 25 Feb 2020

**HAL** is a multi-disciplinary open access archive for the deposit and dissemination of scientific research documents, whether they are published or not. The documents may come from teaching and research institutions in France or abroad, or from public or private research centers.

L'archive ouverte pluridisciplinaire **HAL**, est destinée au dépôt et à la diffusion de documents scientifiques de niveau recherche, publiés ou non, émanant des établissements d'enseignement et de recherche français ou étrangers, des laboratoires publics ou privés.



Distributed under a Creative Commons Attribution - NonCommercial - NoDerivatives 4.0 International License

# Pathogenesis of Hepatic Tumors following Gene Therapy in Murine and Canine Models of Glycogen Storage Disease

Hye-Ri Kang,<sup>1</sup> Monika Gjorgjieva,<sup>2</sup> Stephanie N. Smith,<sup>3</sup> Elizabeth D. Brooks,<sup>1</sup> Zelin Chen,<sup>4</sup> Shawn M. Burgess,<sup>4</sup> Randy J. Chandler,<sup>3</sup> Lauren R. Waskowicz,<sup>1</sup> Kylie M. Grady,<sup>1</sup> Songtao Li,<sup>1</sup> Gilles Mithieux,<sup>2</sup> Charles P. Venditti,<sup>3</sup> Fabienne Rajas,<sup>2</sup> and Dwight D. Koeberl<sup>1</sup>

<sup>1</sup>Division of Medical Genetics, Department of Pediatrics, Duke University School of Medicine, Durham, NC, USA; <sup>2</sup>U1213, Institut National de la Santé et de la Recherche Médicale, Université Lyon 1, Lyon, France; <sup>3</sup>Developmental Genomics Section, Translational and Functional Genomics Branch, National Human Genome Research Institute, Bethesda, MD, USA; <sup>4</sup>Organic Acid Research Section, Medical Genomics and Metabolic Genetics Branch, National Human Genome Research Institute, Bethesda, MD, USA

**Glycogen storage disease type Ia (GSD Ia) is caused by mutations in the glucose-6-phosphatase (G6Pase) catalytic subunit gene (G6PC). GSD Ia complications include hepatocellular adenomas (HCA) with a risk for hepatocellular carcinoma (HCC) formation. Genome editing with adeno-associated virus (AAV) vectors containing a zinc-finger nuclease (ZFN) and a G6PC donor transgene was evaluated in adult mice with GSD Ia. Although mouse livers expressed G6Pase, HCA and HCC occurred following AAV vector administration. Interestingly, vector genomes were almost undetectable in the tumors but remained relatively high in adjacent liver ( $p < 0.01$ ). G6Pase activity was decreased in tumors, in comparison with adjacent liver ( $p < 0.01$ ). Furthermore, AAV-G6Pase vector-treated dogs with GSD Ia developed HCC with lower G6Pase activity ( $p < 0.01$ ) in comparison with adjacent liver. AAV integration and tumor marker analysis in mice revealed that tumors arose from the underlying disorder, not from vector administration. Similarly to human GSD Ia-related HCA and HCC, mouse and dog tumors did not express elevated  $\alpha$ -fetoprotein. Taken together, these results suggest that AAV-mediated gene therapy not only corrects hepatic G6Pase deficiency, but also has potential to suppress HCA and HCC in the GSD Ia liver.**

## INTRODUCTION

Glycogen storage disease type Ia (GSD Ia) is caused by mutations in the *G6PC* gene, leading to the deficiency of glucose-6-phosphatase (G6Pase), the enzyme responsible for maintaining normoglycemia via the dephosphorylation of glucose-6-phosphate (G6P) to produce free glucose.<sup>1</sup> Without G6Pase, a key enzyme in both gluconeogenesis and glycogenolysis, severe hypoglycemia occurs during periods of fasting between meals.<sup>2</sup> Dietary therapy consisting of strictly scheduled uncooked cornstarch consumption has reversed acute symptoms and increased the lifespan of GSD Ia patients;<sup>3,4</sup> however, there has been little progress in reversing hepatocellular abnormalities that lead to long-term complications. Most GSD Ia patients develop hepatomegaly early in life, and 70%–80% of individuals older than 25 have

at least one hepatocellular adenoma (HCA).<sup>5</sup> Approximately 10% of patients with adenomas will develop hepatocellular carcinomas (HCCs) thought to be derived from preexisting adenomas.<sup>6,7</sup> The predominant liver abnormalities in GSD Ia are accumulated glycogen and triglycerides, and the latter represents hepatosteatosis. The hepatosteatosis in GSD Ia might underlie liver tumor formation, given that previous research has shown increased risk of HCC linked to steatosis in patients with non-cirrhotic non-alcoholic fatty liver disease (NAFLD) and type II diabetes.<sup>8</sup> Recent studies have also shown that macroautophagy (referred henceforth as autophagy) is impaired in G6Pase-deficient hepatic cells, both *in vitro* and *in vivo*.<sup>9</sup> Autophagy functions as the cell's recycling system by sequestering damaged organelles and other cytoplasmic components for delivery to the lysosome to be degraded.<sup>10</sup> The deficiency in autophagy has been linked to hepatosteatosis in GSD Ia, and the reversal of hepatosteatosis has been linked to the induction of autophagy in mice with GSD Ia.<sup>9,11</sup> Autophagy-deficient mice tend to develop multiple HCAs and suggest that defective autophagy could contribute to HCA development in GSD Ia.<sup>12</sup> Additionally, metabolic perturbations in GSD Ia associated with the loss of several cellular defenses, such as autophagy, antioxidant enzymes, dysregulation of ER stress responses, and apoptosis, can lead to the formation of HCC.<sup>13</sup>

Gene therapy with adeno-associated virus (AAV) vectors encoding G6Pase have demonstrated efficacy in mice and dogs with GSD Ia, reversing hepatocellular abnormalities to a great extent.<sup>14</sup> Accumulated glycogen was remarkably decreased in the liver of dogs with GSD Ia, in association with decreased hepatic lipids, following administration of an AAV serotype 2 vector cross-packaged as AAV

Received 25 September 2019; accepted 30 October 2019;  
<https://doi.org/10.1016/j.omtm.2019.10.016>

**Correspondence:** Dwight D. Koeberl, Box 103856, Division of Medical Genetics, Department of Pediatrics, Duke University School of Medicine, Duke University Medical Center, Durham, NC 27710, USA.

**E-mail:** [koebe001@mc.duke.edu](mailto:koebe001@mc.duke.edu)



serotype 8 (AAV2/8-G6Pase), and efficacy was maintained for 1 year.<sup>15</sup> We recently described five GSD Ia dogs treated with AAV-G6Pase therapy that survived up to 8 years; however, four of these dogs had hepatocellular tumors, indicating some loss of therapeutic efficacy.<sup>16</sup>

Several experiments have demonstrated that AAV vector administration to young mice accomplished a high level of liver transduction, followed by declining numbers of vector genomes over the ensuing months.<sup>14,17-19</sup> For example, an AAV2/8 vector encoding G6Pase decreased from > 2 copies per liver cell at 1 month of age to 0.3 copies at 7 months of age in *G6pc*<sup>-/-</sup> mice with GSD Ia.<sup>14,15,20</sup> Similarly, an AAV2/8 vector was administered to a GSD Ia puppy at 1 day of age and prevented fasting hypoglycemia for 3 h at 1 month of age; however, by two months of age the dog became hypoglycemic after 1 h of fasting.<sup>18</sup> These data raised the possibility that the biochemical correction from transduction of the liver with AAV vectors might decrease over time, with the accompanying risk that efficacy might be diminished. Indeed, Lee et al.<sup>20</sup> reported that > 90% of G6Pase activity was lost between 6 and 18 months following administration of an AAV2/8 vector encoding G6Pase to neonatal *G6pc*<sup>-/-</sup> mice, but also that hypoglycemia and HCC formation was prevented by only 3% of normal G6Pase activity in the liver. Long-term monitoring of *G6pc*<sup>-/-</sup> mice following administration of an AAV2/9 vector encoding G6Pase at 2 weeks of age revealed persistence of transgene expression in only a small fraction of cells, suggesting that the great majority of hepatocytes remain uncorrected following AAV vector-mediated gene replacement.<sup>21</sup>

Earlier experiments demonstrated the need for more complete and persistent correction of G6Pase deficiency in the GSD Ia liver, which has motivated us to develop a genome-editing strategy to more stably replace G6Pase and more effectively prevent tumor formation in the liver.

We have developed a zinc-finger nuclease (ZFN) targeted to the *ROSA26* gene in mice to insert a transgene into a safe harbor locus and stably correct the G6Pase deficiency in GSD Ia.<sup>22</sup> Administration of two AAV2/9 vectors (cross-packaged as AAV9), one containing the ZFN and one containing a *ROSA26*-targeting vector containing a *G6PC* donor transgene, markedly improved survival in *G6pc*<sup>-/-</sup> mice through stable G6Pase expression in liver. However, HCC have not been observed in untreated *G6pc*<sup>-/-</sup> mice as old as 6 months, which limits the usefulness of this model for studying the prevention of HCC.<sup>23</sup> Based on these results, we have investigated whether a genome-editing-based correction approach with these two vectors can suppress hepatic tumors in the adult liver-specific *G6pc*<sup>-/-</sup> mouse model (L-*G6pc*<sup>-/-</sup>), a model that consistently formed HCC by 1 year of age.<sup>24</sup>

## RESULTS

### Suppression of Hepatic Tumors with G6Pase Expression in the L-*G6pc*<sup>-/-</sup> Mouse and Canine Models

We administered AAV vectors to perform ZFN-mediated genome editing in L-*G6pc*<sup>-/-</sup> mice, with the goal of preventing hepatic tu-

mor formation in the GSD Ia liver. The vectors, AAV2/9-ZFN (ZFN-containing) and AAV2/9-RoG6P (*G6PC* donor-containing) were administered to L-*G6pc*<sup>-/-</sup> mice at 7–8 weeks of age, following liver *G6pc* deletion induced by tamoxifen injection at 3 weeks of age as described.<sup>24</sup> The *G6PC* donor vector is designed to integrate at the *Rosa26* locus, once cleaved by the ZFN, following administration of dual vectors.<sup>22</sup> Dual vector-treated mice were compared with groups of mice that received the ZFN-containing or donor-containing vector alone. The ZFN group was essentially untreated, because no *G6PC* transgene was delivered to correct G6Pase deficiency. The donor group had no effect on genome editing, because no ZFN was present to produce double-stranded breaks at the *Rosa* locus.<sup>22</sup> The effect of genome editing following AAV vector administration was evaluated by measuring liver weight, G6Pase activity, glycogen accumulation, triglycerides, nuclease activity, transgene integration, and *G6PC* vector DNA, as well as blood glucose during a 12-month period following dual vector administration (Figure S1). These data indicated that the effect of ZFN-mediated genome editing with dual vectors was similar to gene replacement with the *G6PC* donor vector in adult L-*G6pc*<sup>-/-</sup> mice, when groups of both sexes were evaluated.

Genome editing in *G6pc*<sup>-/-</sup> mice has been more efficacious in male than in female mice, and therefore the data was analyzed to examine sex-related differences.<sup>22</sup> Only ZFN+*G6PC*-treated male mice showed significantly decreased liver mass in comparison with the ZFN group (Figures 1A and 1B). Trends toward greater biochemical correction, including G6Pase activity (Figure 1C), hepatic glycogen accumulation (Figure 1D), and triglyceride content (Figure 1E), were demonstrated in ZFN+*G6PC*-treated males, in comparison with females. Both *G6PC*- and ZFN+*G6PC*-treated male mice demonstrated improved blood glucose levels in comparison with ZFN-treated male mice (Figure 1F). Comparisons of *G6PC*- and ZFN+*G6PC*-treated male mice revealed further improvement from genome editing through 12 months of observation. Female mice demonstrated improved blood glucose at fewer time points in comparison with ZFN-treated female mice (Figure 1G). Therefore, the biochemical correction of the liver with genome editing was more effective in male mice.

Despite increased G6Pase activity, the dual vector-treated group still developed hepatic tumors (6 out of 14), although in slightly lower numbers in comparison with the *G6PC* donor (8 out of 12) and ZFN groups (4 out of 8) without reaching statistical significance. Similarly, the number of tumors per mouse in the dual vector group (0.7 per mouse) was slightly lower than in other groups (> 0.9 per mouse). Importantly, we found that tumors lacked AAV vector genomes ( $p < 0.01$ ) in comparison with adjacent normal liver tissue (Figure 2A). Consistent with the presence of fewer vector genomes, tumors had decreased G6Pase activity ( $p < 0.05$ ) in comparison with the adjacent liver (Figure 2B). However, there was no difference in glycogen content between liver and tumor tissue (Figure 2C). Analysis of low-molecular-weight Hirt DNA fraction to detect episomal AAV vector genomes revealed that tumors also lacked episomal

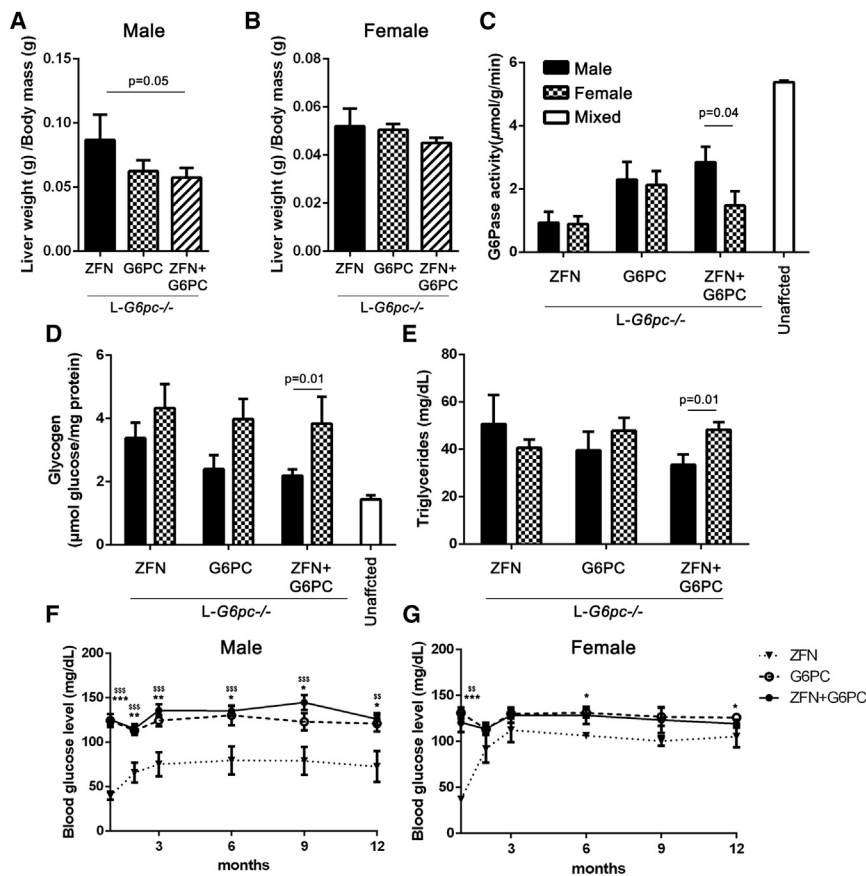


**Figure 1. Gender Differences in Biochemical Correction of Liver**

(A and B) Analysis of liver weight normalized by body mass and by sex differences. (A) Male (ZFN,  $n = 5$ ; G6PC,  $n = 7$ ; ZFN+G6PC,  $n = 9$ ) and (B) female (ZFN,  $n = 3$ ; G6PC,  $n = 5$ ; ZFN+G6PC,  $n = 5$ ). Data depicted as means  $\pm$  SEM.  $p$  values from  $t$  test. (C–E) Male mice of the ZFN+G6PC group showed significantly higher (C) G6Pase activity, (D) lower glycogen accumulation, and (E) lower triglycerides levels compared to same-treated female mice. No correction was shown in female mice. Numerical  $p$  values from  $t$  test. (F and G) Blood glucose levels were measured after 6 hours fasting through 12 months in both male mice (F) and female mice group (G). Numbers of mice per each group are ZFN male ( $n = 5$ ), ZFN female ( $n = 3$ ), G6PC male ( $n = 4$ ), G6PC female ( $n = 6$ ), ZFN+G6PC male ( $n = 9$ ), and ZFN+G6PC female ( $n = 5$ ). Data depicted as means  $\pm$  SEM. \* $p < 0.05$ , \*\* $p < 0.005$ , \*\*\* $p < 0.0005$  from  $t$  test between ZFN and G6PC group.  $^{\$}p < 0.05$ ,  $^{\$\$}p < 0.005$ ,  $^{\$\$\$}p < 0.0005$  from  $t$  test between ZFN and ZFN+G6PC group.

vector genomes (Figures 2D and 2E). In contrast, liver adjacent to tumors retained episomal vector genomes (Figures 2D and 2E).

We subsequently quantified the effects of genome editing in dual vector-treated mice to allow comparisons between those with no tumors and those with tumors. The ZFN was more active in the no-tumor group, suggesting a beneficial effect of genome editing. The activity of the ZFN was analyzed with the Surveyor nuclease assay performed on liver genomic DNA. The average allele modification (insertions and deletions [indels]) rate was 4.5% following genome editing, while the tumor group was 0.9% ( $p = 0.03$ ; Figure 2F). No transgene integration was present in available tumor DNA samples (Figure 2G). In contrast, transgene integration was detected in 9 of 12 liver samples from the ZFN+G6PC group (Figure S1B). In addition, the male no-tumor group had G6Pase activity equivalent to unaffected mice, whereas the male tumor group had significantly decreased G6Pase activity (Figure 2H). Analysis of female mice revealed no difference in G6Pase activity between groups (data not shown). These results suggest that sufficient G6Pase expression could prevent tumor formation in transduced GSD Ia liver.

The canine GSD Ia model has features similar to human GSD Ia, including lactic acidemia and a high risk for developing HCA.<sup>16,25</sup> To verify that the same phenotype exists in the canine GSD Ia dogs

with hepatocellular tumors, we compared G6Pase activity and glycogen content between tumors and the adjacent liver. These dogs were treated with the AAV2/9- or AAV2/8-G6Pase vector without genome editing at birth and required periodic re-administration of vector cross-packaged with different AAV serotypes throughout their lives to control GSD symptoms.<sup>26</sup> G6Pase activity was increased following vector administration, in comparison with untreated liver ( $p < 0.05$ ). Consistent with the data from  $L-G6pc^{-/-}$  mice, the tumors had lower G6Pase activity, in comparison with adjacent liver ( $p < 0.05$ ,  $t$  test; Figure 3A). Glycogen content was increased in the tumors, in comparison with the adjacent liver, without reaching statistical significance (Figure 3B). Histochemical staining for G6Pase expression revealed increased G6Pase in liver in comparison with the tumors (Figures 3C–3F). Taken together, these results suggest that the expression of G6Pase with an AAV vector was associated with the absence of tumor in the canine GSD Ia liver.

#### Analysis of AAV Integration and Tumorigenesis

To gain insight into whether AAV vector-mediated tumorigenesis might contribute to HCA/HCC formation in the treated GSD mice, we evaluated AAV integration profiles and selected biomarkers in HCCs isolated from vector-treated neonatal mice.<sup>27</sup> It has been well established that the absence of AAV vector genomes from tumor DNA (Figures 2A, 2D, and 2E) does not eliminate the possibility that vector integrations can contribute to HCC formation in mice, since the integration of promoter and enhancer sequences alone can drive tumorigenesis without the presence of other vector genome sequences.<sup>28–30</sup> AAV vector integrations were detected using a sensitive high-throughput integration site-capture technique, and events at the *Rian* locus, which has been identified in numerous studies as a risk

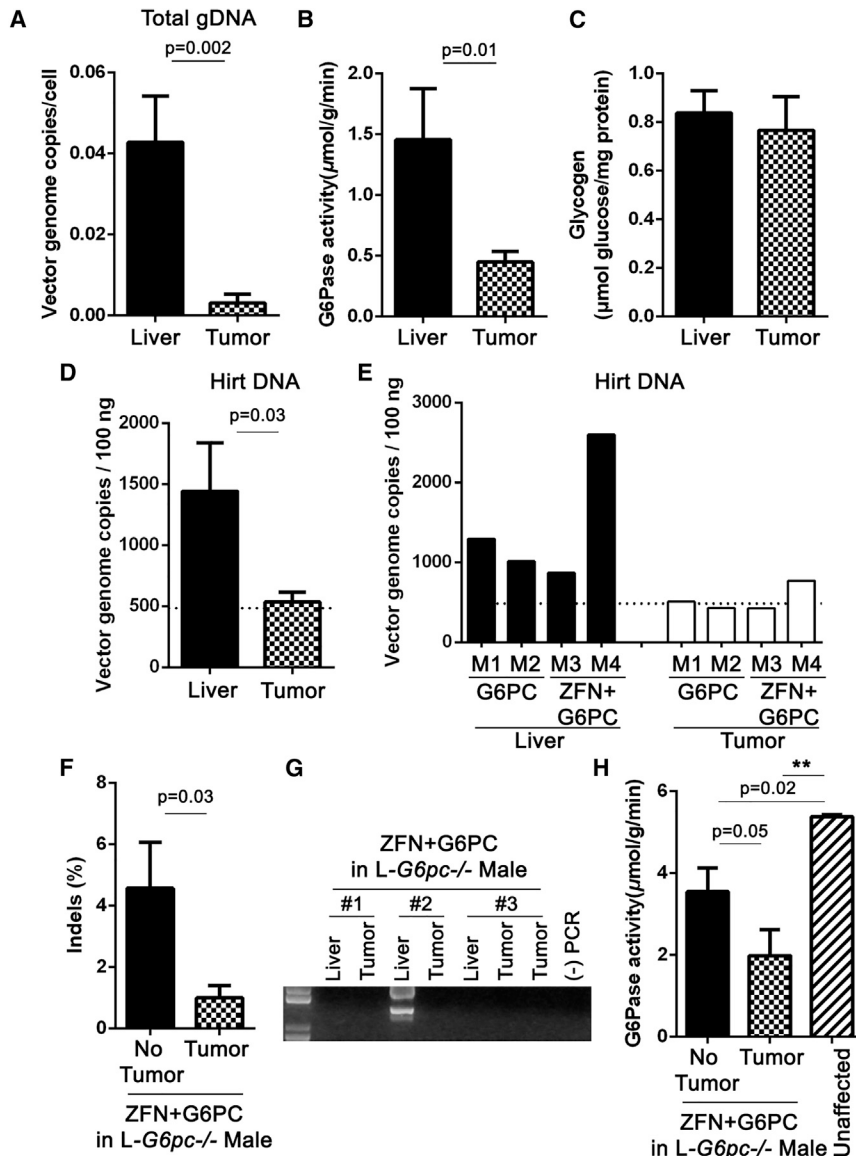


**Figure 2. Analysis of Hepatic Parameters between Adjacent Liver and Tumor of L-G6pc<sup>-/-</sup> Mice after AAV Administration**

(A) Genomic DNAs were extracted from tumors ( $n = 6$ ) and adjacent livers ( $n = 5$ ) in each mouse. Donor vectors were quantified and compared between them. Donor vectors were almost lost in tumor in comparison with adjacent liver. (B and C) Hepatic G6Pase activity (B) and glycogen accumulation (C) were measured. G6Pase activity of tumor was significantly lower than adjacent liver, but glycogen accumulation levels did not differ between groups. (D and E) Low-molecular Hirt DNAs were extracted from tumors ( $n = 4$ ) and adjacent livers ( $n = 4$ ). Donor vectors were quantified and compared between them. (D) Tumor lacked donor vector genomes in comparison with adjacent liver. (E) Each bar indicates donor vector genome from each mouse. (F and H) ZFN activity (indel %) (F) and G6Pase activity (H) was measured in male group treated with dual vectors. Numbers of mice per each group are as follows: no tumor ( $n = 5$ ), tumor ( $n = 4$ ), and unaffected ( $n = 3$ ). (G) Transgene integration was analyzed in tumors ( $n = 4$ ) and adjacent liver ( $n = 3$ ). Data depicted as means  $\pm$  SEM. \* $p < 0.05$ , \*\* $p < 0.01$ , \*\*\* $p < 0.001$ , \*\*\*\* $p < 0.0001$  from ANOVA and numerical  $p$  values from t test.

formed after AAV vector integration.<sup>27</sup> In contrast to what has been observed with AAV-associated HCCs in other studies, the expression of neither *Rtl1* nor *Mir543* were elevated in the tumors, supporting the hypothesis that the HCCs developed as a complication of GSD, not AAV vector integration (Figures 4B–4D).<sup>27</sup> AFP is not elevated in GSD Ia-related HCC in humans,<sup>6,7</sup> but AFP was markedly elevated in HCC related to AAV insertional mutagenesis.<sup>27</sup> One tumor had moderately elevated *Afp* expression, which has been reported in HCC caused by GSD Ia in the L-G6pc<sup>-/-</sup> mice without AAV administration (Figure 4B).<sup>13</sup> Given the lack of elevation of *Rtl1* and *Mir543* expression and the moderate elevation of *Afp*, it is more likely that tumorigenesis in mice was related to GSD Ia. The presence of AFP was analyzed in GSD Ia dog tumors to determine whether the etiology of HCC formation was more likely related to GSD Ia (low AFP)<sup>6,7</sup> or to AAV vector administration (high AFP)<sup>27</sup> (Figure 5). RT-PCR revealed absent *Afp* expression in canine HCC samples (Figure 5A), which correlated with absent AFP on immunoblotting (Figure 5B). In contrast, neonatal canine liver revealed increased *Afp* expression by RT-PCR as expected (Figure 5A), which confirmed the ability to detect *Afp* expression. Immunohistochemistry revealed the presence of AFP in neonatal liver and its absence in canine GSD Ia HCC and normal liver (Figure 5C). The absence of AFP in canine GSD Ia HCC confirmed that GSD Ia was the most likely etiology.<sup>6,7</sup>

factor for HCC development after AAV integration in mice, were analyzed in greater detail.<sup>27</sup> When both the tumors and adjacent unaffected liver were analyzed, only five integrations were deemed high risk based upon integration at the *Rian* locus and a high fragment count, and three of those five were detected in adjacent liver as opposed to the tumor tissue (Table 1). These high-risk *Rian* locus integrations were detected in two of 10 tumors and three of 27 unaffected liver samples analyzed. Integration events mapped near the genomic location of integration events identified in HCCs isolated from mice after treatment with high doses of AAV during the neonatal period (Figure 4A).<sup>27</sup>

We next quantified *Afp*, *Rtl1*, and *Mir543* expression in tumor samples, because these markers have been identified in HCCs that

formed after AAV vector integration.<sup>27</sup> In contrast to what has been observed with AAV-associated HCCs in other studies, the expression of neither *Rtl1* nor *Mir543* were elevated in the tumors, supporting the hypothesis that the HCCs developed as a complication of GSD, not AAV vector integration (Figures 4B–4D).<sup>27</sup> AFP is not elevated in GSD Ia-related HCC in humans,<sup>6,7</sup> but AFP was markedly elevated in HCC related to AAV insertional mutagenesis.<sup>27</sup> One tumor had moderately elevated *Afp* expression, which has been reported in HCC caused by GSD Ia in the L-G6pc<sup>-/-</sup> mice without AAV administration (Figure 4B).<sup>13</sup> Given the lack of elevation of *Rtl1* and *Mir543* expression and the moderate elevation of *Afp*, it is more likely that tumorigenesis in mice was related to GSD Ia. The presence of AFP was analyzed in GSD Ia dog tumors to determine whether the etiology of HCC formation was more likely related to GSD Ia (low AFP)<sup>6,7</sup> or to AAV vector administration (high AFP)<sup>27</sup> (Figure 5). RT-PCR revealed absent *Afp* expression in canine HCC samples (Figure 5A), which correlated with absent AFP on immunoblotting (Figure 5B). In contrast, neonatal canine liver revealed increased *Afp* expression by RT-PCR as expected (Figure 5A), which confirmed the ability to detect *Afp* expression. Immunohistochemistry revealed the presence of AFP in neonatal liver and its absence in canine GSD Ia HCC and normal liver (Figure 5C). The absence of AFP in canine GSD Ia HCC confirmed that GSD Ia was the most likely etiology.<sup>6,7</sup>

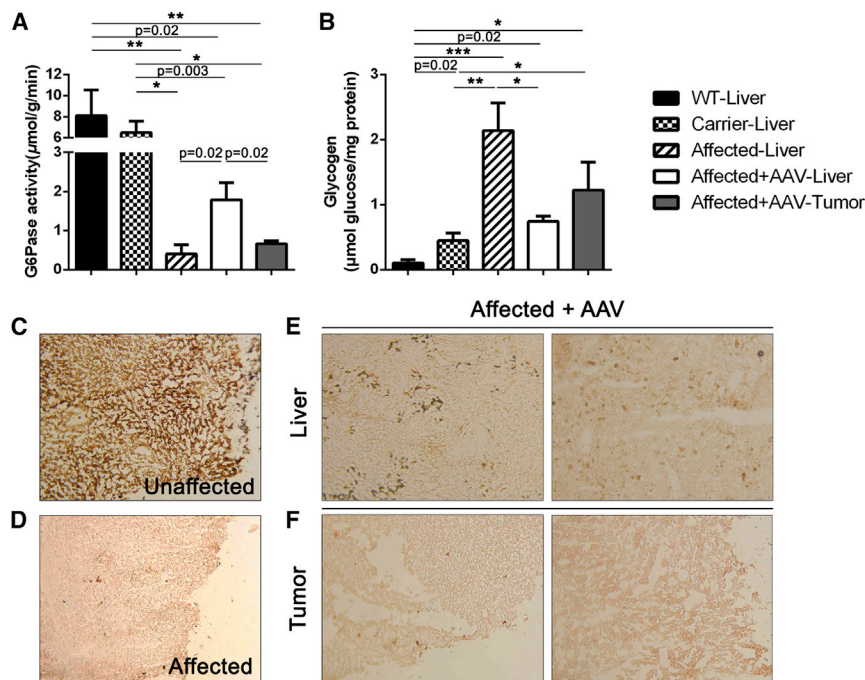


**Figure 3. Biochemical Correction of Tumors and Adjacent Liver for GSD Ia Dogs after AAV Administration**

GSD Ia-affected dogs ( $n = 4$ ) were treated with G6PC. WT ( $n = 4$ ), carrier ( $n = 5$ ), and affected without AAV ( $n = 3$ ) dogs were used as a control groups. (A and B) Hepatic G6Pase activity (A) and glycogen accumulation (B) were measured. After AAV administration, glycogen level was decreased, which correlated with higher G6Pase activity in livers of affected dogs. G6Pase activity of tumor was significantly lower than adjacent liver, but glycogen accumulation levels did not differ between groups. (C–F) Representative G6Pase staining sections from unaffected (C), GSD Ia-affected (D), adjacent liver (E), and tumor (F). Dark brown spots indicate positive G6Pase staining. Tumor sections featured significantly reduced G6Pase staining spot compared to adjacent liver. Data depicted as means  $\pm$  SEM. \* $p < 0.05$ , \*\* $p < 0.01$ , \*\*\* $p < 0.001$ , \*\*\*\* $p < 0.0001$  from ANOVA and numerical  $p$  values from  $t$  test.

## DISCUSSION

Here, we present ZFN-mediated genome editing with dual AAV vectors in adult mice with GSD Ia, which decreased GSD Ia-related tumor formation in the liver. AAV vector genomes were almost undetectable in the tumors but remained relatively high in the adjacent liver. We also found that hepatocellular tumors in the AAV vector-treated GSD Ia canine model contained lower G6Pase activity in comparison with adjacent liver. Overall, this study and others support the prevailing hypothesis that sufficient G6Pase expression will prevent HCA/HCC in GSD Ia.<sup>31,32</sup>

Previous studies of AAV vector-mediated gene therapy in universal *G6pc*<sup>-/-</sup> mice revealed a threshold of 3% of normal G6Pase activity to prevent tumor formation in the liver,<sup>20,31</sup> which contrasts with the high rate of tumor occurrence despite stable restoration of significant G6Pase activity with an efficacious genome-editing strategy delivered by AAV vectors in this study. The earlier age of vector administration in the neonatal period might have been protective against tumor formation in previous studies,<sup>20,31</sup> in contrast to vector administration to adult mice in the current study. Furthermore, the presence of HCC in the dog model treated with non-integrating AAV vectors emphasized that the gradual loss of vector genomes over several years increased the risk of tumor formation, which could not be demonstrated in the mouse models due to their relatively short lifespan. While long-term G6Pase activity was increased in the vector-treated GSD Ia dogs, it did not approach the same levels as that detected in carrier or wild-type dogs. G6Pase activity was sufficient to improve survival, but not to prevent tumor formation.<sup>16</sup> Another long-term study of gene therapy in the same GSD Ia dog model re-

ported no liver tumor formation; however, intensive nutritional management was the best explanation for tumor prevention in that study, because two GSD Ia dogs treated with nutrition alone (and no gene therapy) developed no tumors in more than 5 years of observation.<sup>33,34</sup>

Another risk factor for HCC in mice with GSD Ia has not been addressed following gene therapy—namely, the known risk for tumorigenesis related to AAV vector genotoxicity. Previous studies demonstrated a high risk for HCC formation following administration of AAV vectors to neonatal mice,<sup>27,28</sup> although one study revealed an increased risk of tumorigenesis among a large group of adult mice.<sup>35,36</sup> These studies implicated an *rAAV-HCC* locus in rodents, which stems from AAV integration in the *Rian* locus and the upregulation of the *Rtl1* gene.<sup>27,36</sup> AAV integrations across the entire 58-kb *Rian* locus have been associated with HCC.<sup>37</sup> While *Rian* AAV integrations were currently detected in tumors from mice with GSD Ia, we did not find the upregulation of genes that have been associated with HCC following integrations into *Rian* locus.<sup>27,28</sup> These data suggested that the *Rian* integrations were not the cause of the tumors in the GSD mice. It is possible that the tissue-specific promoters included in our vectors, the liver-specific promoter (LSP) and minimal *G6PC* promoters, failed to activate the *Rian* locus, as has been described for a human alpha 1-antitrypsin promoter.<sup>27</sup> Furthermore, AAV integrations into *Rian* that did not result in HCC have been reported, and other factors, such as the nature of the enhancers and promoters, appear to be important determinants as to whether these integrations will result in oncogenesis.<sup>27,29</sup> One of these tumors did have increased expression of *Afp*, which is upregulated in some types of HCC, including those in murine GSD Ia.<sup>13</sup> Whether this tumor is

**Table 1. AAV Integrations at the *Rian* Locus**

Treatment	Tissue	Integration Start	Sequenced Fragment Count
Donor	liver	109,606,646	518
Donor	liver	109,625,075	2,410
Donor	liver	109,631,802	4,162
ZFN	tumor	109,635,601	2,820
Dual vector	tumor	109,615,611	7,236

naturally occurring or associated with a non-*Rian* genotoxic AAV integration or perhaps a sporadic event is unclear, but the aggregate results suggest that AAV gene delivery does not increase the risk of HCC formation in L-*G6pc*<sup>-/-</sup> mice that has been previously attributed to G6Pase deficiency.<sup>24</sup> Furthermore, analysis of HCC from GSD Ia dogs treated with AAV vectors did not reveal elevated AFP, consistent with an etiology of GSD Ia.<sup>6,7</sup>

Although our gene-therapy experiments were not designed to specifically examine rAAV hepatocarcinogenic effects and did not incorporate parallel transcriptomic/genomic analyses or survey HCC in large cohorts of mice to assess the strain-dependent rate of HCC formation, the aggregate results provide independent support for the hypothesis that AAV-mediated gene therapy, via the correction of hepatic G6Pase deficiency, has the potential to suppress tumor formation in the GSD Ia liver.<sup>38</sup> These data are consistent with previously published data in the *G6pc*<sup>-/-</sup> mouse model.<sup>20,31</sup>

This study replicated a sex-related difference in the response to genome editing in mice with GSD Ia, previously reported in the neonatal *G6pc*<sup>-/-</sup> model.<sup>22</sup> Administration of both the ZFN and *G6PC* donor increased G6Pase activity in liver of male mice, in comparison with the ZFN alone, but not in the population of both sexes. These data indicated that genome editing with dual vectors containing the ZFN and *G6PC* donor was not efficacious in the adult female L-*G6pc*<sup>-/-</sup> model for GSD Ia. Female L-*G6pc*<sup>-/-</sup> mice presented with a milder phenotype, as shown by greater resistance to hypoglycemia in comparison with males (Figures 1F and 1G). However, the degree of biochemical correction in the liver following genome editing was clearly improved in males, which confirmed that females had decreased benefits from genome editing (Figures 1C–1E). One potential explanation for this effect is the greater transduction efficiency of AAV vectors in male mice in comparison with female mice.<sup>39–41</sup>

Despite the incidence of HCC in this study, the loss of the *G6PC* transgene from the tumor and presence in adjacent liver suggested a reduced risk for tumor formation from G6Pase transduction in the GSD Ia liver.

## MATERIALS AND METHODS

### Preparation of AAV Vectors

The AAV vector plasmid pAAV-RoG6P contained the vector gene comprised of a terminal repeat (TR) at each end flanking a transgene

comprised of the human G6Pase minimal promoter to drive a human G6Pase cDNA followed by a human growth hormone polyadenylation signal, which was flanked by sequences from exon 1 of the mouse *Rosa26* locus.<sup>42</sup> The G6Pase-encoding transgene was previously described.<sup>15</sup> The AAV vector plasmid, pAAV-ZFN, contained the transgene for the two subunits of the ROSA26-targeting “R4L6 eZFN,”<sup>43</sup> separated by a T2A self-cleavage peptide and expressed from the LSP and flanked by TR sequences. AAV vectors were packaged as described.<sup>22</sup>

### Animal Use

GSD dogs received human care, and animal studies were approved by Duke University Institutional Animal Care and Use Committee. GSD Ia-affected dogs treated with a non-integrating vector encoding *G6PC*, AAV-G6Pase, were followed up to 8 years of age.<sup>16</sup> All required readministration of AAV vector(s), pseudotyped as a new serotype to avoid anti-AAV antibodies, due to decreased ability to maintain normoglycemia during fasting.<sup>26</sup> Dogs with tumors were euthanized due to reaching humane endpoints related to liver and/or kidney involvement at 3 to 8 years of age. Complete necropsies were performed on all dogs and tissues were frozen, flash frozen in Tissue-Tek OCT compound (Sakura Finetek, Torrance, CA, USA), or fixed in 10% neutral-buffered formalin and stored at -80°C or 4°C, respectively. Multiple tissues including liver and kidneys were examined from all dogs.

Liver *G6pc*<sup>-/-</sup> mice were injected intravenously with vectors: 1.3E+13 vector genomes (vg)/kg AAV2/9-RoG6P and 4.8E+12 vg/kg AAV2/9-ZFN at 7–8 weeks of age, following the induction of liver *G6pc* deletion at 3 weeks of life by tamoxifen injection, and the mice were monitored for 12 months of age as described.<sup>24</sup>

All procedures involving mice were performed in accordance with the principles and guidelines established by the European Convention for the Protection of Laboratory Animals. The animal care committee of University of Lyon approved all the mouse experiments.

### Quantification of DNA Repair at the *Rosa26* Locus in the Liver

Liver DNA was extracted using the Wizard genomic DNA purification kit (Promega, Madison, WI, USA). The *Rosa26* locus was PCR-amplified and the Surveyor nuclease assay (Transgenomic, Omaha, NE, USA) was performed as described.<sup>22</sup>

### Low-Molecular-Weight Hirt DNA Preparation

Liver and tumor Hirt DNA were prepared according to a previously published protocol,<sup>44</sup> with several modifications. Specifically, 20 mg of liver or tumor tissue was homogenized in 600 μL lysis buffer (10 mM Tris-Cl [pH 8.0], 10 mM EDTA, 1% SDS, and 1 μL of DNase-free 10 mg/mL RNase A) and was incubated at 37°C for 1 h. 1 mg/mL Proteinase K was added to the mixture, and mixture was incubated at 37°C for 2 h. Following incubation, NaCl was added to the mixture at a final concentration of 1.1 M. After overnight incubation at 4°C, samples were centrifuged at 14,000 rpm for 30 min, and

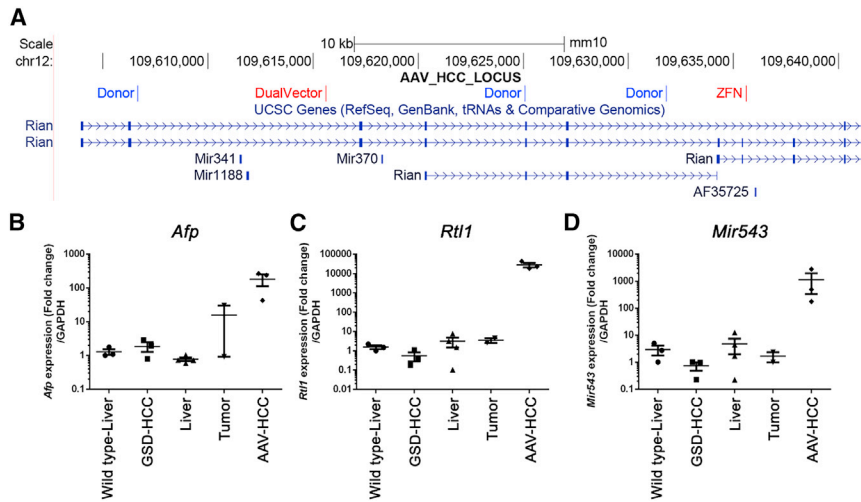


**Figure 4. AAV Integration and HCC Marker Analysis in Tumors and Liver**

(A) Integration of AAV vectors in the *Rian* locus. Mice were treated with the donor vector (AAV2/9-RoG6P), dual vectors (AAV2/9-ZFN and AAV2/9-RoG6P), or ZFN (AAV2/9-ZFN). Tumor samples indicated in red text, and adjacent liver samples indicated in blue text. (B–D) Expression of *Afp* (B), *Rtl1* (C), and *Mir543* (D) from wild-type liver, HCC from untreated L-G6pc<sup>-/-</sup> mice<sup>13</sup> (GSD-HCC), AAV-treated GSD la liver (liver), AAV-treated GSD la tumors (tumor), and AAV-related HCC<sup>27</sup> (AAV-HCC) were determined by real-time PCR.

#### Detection of AAV Integration and HCC Markers in Tumors and Liver

Integration detection by Ligation mediated-PCR, mapping and annotation, and real-time PCR of HCC markers were performed as described.<sup>27</sup> Total

RNA was extracted for real-time PCR and purified using Trizol reagent transcriptase (Thermo Scientific, Waltham, MA, USA) combined with Direct-zol RNA miniprep kit (Zymo Research, Irvine, CA, USA), and cDNA was synthesized using a high-capacity cDNA reverse transcription kit (Thermo Scientific, Waltham, MA, USA). qPCR was performed with a QuantStudio 5 real-time PCR machine using Taqman assays (Applied Biosystems/Thermo Scientific, Waltham, MA, USA) for *Afp*, *Rtl1*, *Mir543*, and *Gapdh* (assay no. Mm00431715\_m1, Mm02392620\_s1, Mm04238293\_s1, and Mm9999915\_g1, respectively). Relative expression was calculated using the  $\Delta\Delta C_t$  method.

#### Immunoblotting

Western blotting was performed as described.<sup>11</sup> Tris/glycine/SDS running buffer (161-0732; Bio-Rad Laboratories, Hercules, CA, USA), polyvinylidene fluoride (PVDF; 162-0177; Bio-Rad Laboratories, Hercules, CA, USA), and ECL substrate reagent (34095; Thermo Fisher Scientific, Waltham, MA, USA) were used. Primary antibodies for  $\alpha$ -fetoprotein (AFP) (ab 231264; Abcam, Cambridge, MA, USA),  $\beta$ -actin (A3854; Sigma, St. Louis, MO, USA), and  $\alpha$ -rabbit immunoglobulin G (IgG)-conjugated horseradish peroxidase (Santa Cruz) were used.

#### Immunohistochemistry (IHC)

Hepatic tissues were fixed in 10% neutral buffered formalin, processed routinely to paraffin, sectioned at 5  $\mu$ m, and immunostained for reactivity for  $\alpha$ -fetoprotein using a rabbit polyclonal antibody known to work in canine tissue. The AFP antibody (DAKO A0008; Agilent Technologies, Santa Clara, CA, USA) was used at 1:1,000 dilution and detected with EnVision+ horseradish peroxidase (HRP)-labeled polymer anti-rabbit (DAKO K4003; Agilent Technologies, Santa Clara, CA, USA) after antigen retrieval in citrate buffer (pH 6.1) for 20 min at 100°C.

#### Statistical Analysis

All data are shown as mean  $\pm$  SEM. The mean values of data were compared by ANOVA for comparisons between multiple groups.

Hirt DNA was purified from the supernatants by standard phenol-chloroform extraction and ethanol precipitation.

#### Identification of Transgene/Mouse-Gene Junctions

Genomic DNA was extracted from mouse liver as described above. The PCR reactions with Taq (QIAGEN, Venlo, Limburg, Germany) were performed as described.<sup>22</sup>

#### Quantification of Vector DNA in the Liver

Quantitative real-time PCR was performed using SYBR green in a LightCycler 480II (Roche, Basel, Switzerland) following the manufacturer's instructions as described.<sup>22</sup>

#### Evaluation of Biochemical Correction

G6Pase enzyme analysis was performed as previously described on liver tissues collected at necropsy.<sup>21</sup> Tissues were frozen and stored at  $-80^\circ\text{C}$ . G6Pase activity was quantified by using glucose-6-phosphate (Sigma, St. Louis, MO, USA) as substrate after subtraction of nonspecific phosphatase activity as estimated by glycerol 2-phosphate disodium salt hydrate (Sigma, St. Louis, MO, USA). G6Pase was assessed qualitatively in flash-frozen sections of dog liver by an optimized cerium-diaminobenzidine method as described.<sup>16</sup> Glycogen content was measured by complete digestion of polysaccharide using amyloglucosidase (Sigma, St. Louis, MO, USA). The structure of the polysaccharide was inferred by using phosphorylase free of the debranching enzyme to measure the yield of glucose-1-phosphate.

#### Quantification of mRNA Expression in Mouse and Dog Tissue

Quantitative real-time PCR was performed on cDNA reverse transcribed from total RNA collected from mouse and dog liver tissue as described.<sup>22</sup> Primers for canine tissue were as follows: AFP-F-5'-ggattctccaatgttctgcag-3'; AFP-R-5'-ggtgccttctgctatctcatag-3';  $\beta$  actin-F-5'-gatgacgatcgtcgccttg-3';  $\beta$  actin-R-5'-catcagatgc-cagtggcgg-3'. Relative expression was calculated using the  $\Delta\Delta C_t$  method.<sup>45</sup>

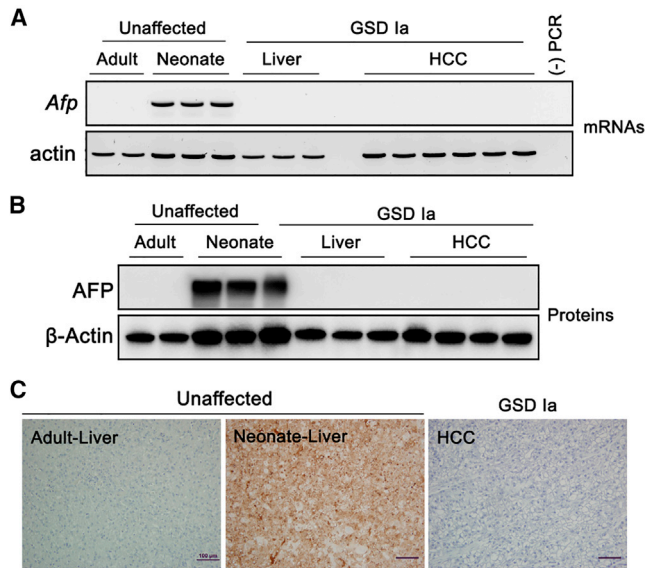


**Figure 5.  $\alpha$ -fetoprotein Expression in Dog Tumors and Liver**

(A and B) *Afp* mRNA level (A) and AFP protein expression (B) were measured in tumors (HCC) of GSD Ia-affected dogs ( $n = 6, 4$ ) and liver of GSD Ia ( $n = 3$ ). (C) Immunohistochemical (IHC) staining of tumor for AFP expression. Brown color indicates AFP expression. Unaffected adult liver ( $n = 2$ ) was used as a negative control group and neonates ( $n = 3$ ) were used as a positive control group.

p values less than 0.05 were considered statistically significant. \* $p < 0.05$ , \*\* $p < 0.01$ , \*\*\* $p < 0.001$ .

#### SUPPLEMENTAL INFORMATION

Supplemental Information can be found online at <https://doi.org/10.1016/j.omtm.2019.10.016>.

#### AUTHOR CONTRIBUTIONS

H.-R.K. performed research on tissue samples, analyzed data, and wrote the paper. M.G. performed experiments with mice and tissue samples and analyzed data. S.N.S. performed research on tissue samples, analyzed data, and wrote the paper. E.D.B. performed experiments with dogs and tissue samples, analyzed data, and wrote the paper. Z.C. analyzed data. S.M.B. analyzed data. R.J.C. performed research on tissue samples, analyzed data, and wrote the paper. L.R.W. performed research on tissue samples and analyzed data. K.M.G. performed experiments with dogs and tissue samples and analyzed data. S.L. performed experiments with dogs and tissue samples and analyzed data. G.M. performed experiments with mice and tissue samples and analyzed data. C.P.V. analyzed data and wrote the paper. F.R. analyzed data and wrote the paper. D.D.K. analyzed data and wrote the paper.

#### CONFLICTS OF INTEREST

D.D.K. served on a data and safety monitoring board for Baxter International. He was supported by R01DK105434-03 from the National Institute of Diabetes and Digestive and Kidney Diseases. He received

an honorarium and grant support in the past from Genzyme Sanofi. None of the other authors had a conflict of interest to declare.

#### ACKNOWLEDGMENTS

We acknowledge funding for this work provided by the Children's Fund for GSD Research, Children's Miracle Network, Association for Glycogen Storage Disease, For the Love of Christopher, the Alice and YT Chen Center for Pediatric Genetics and Genomics, the French National Agency of Research (ANR-11-BSV1-009 to F.R.), Association Francophone des Glycogénoses, and grant R01DK105434-03 (to D.D.K.) from the National Institute of Diabetes and Digestive and Kidney Diseases. S.N.S., R.J.C., Z.C., S.M.B., and C.P.V. were supported by the intramural research program of the National Human Genome Research Program at the NIH and acknowledge sequencing support from the National Intramural Sequencing Center. We would also like to acknowledge inspiration and support from Dr. Emory and Mrs. Mary Chapman and their son Christopher and from Dr. John and Mrs. Michelle Kelly. We wish to acknowledge Ms. Emma Weitzhandler and Ms. Danielle Holdner for technical support. We appreciate the care that the dogs received from the North Carolina State University and Duke University Laboratory Animal Resources staff, as well as the collective support from the multiple students and staff in the dog-feeding team. H.-R.K. was funded by a Pfizer NC Biotechnology Gene Therapy fellowship (agreement GTF-A-4026).

#### REFERENCES

1. Lei, K.J., Chen, H., Pan, C.J., Ward, J.M., Mosinger, B., Jr., Lee, E.J., Westphal, H., Mansfield, B.C., and Chou, J.Y. (1996). Glucose-6-phosphatase dependent substrate transport in the glycogen storage disease type-Ia mouse. *Nat. Genet.* *13*, 203–209.
2. Héron, B., Mikaeloff, Y., Froissart, R., Caridade, G., Maire, I., Caillaud, C., Levade, T., Chabrol, B., Feillet, F., Ogier, H., et al. (2011). Incidence and natural history of mucopolysaccharidosis type III in France and comparison with United Kingdom and Greece. *Am. J. Med. Genet. A.* *155A*, 58–68.
3. Wolfsdorf, J.L., and Crigler, J.F., Jr. (1997). Cornstarch regimens for nocturnal treatment of young adults with type I glycogen storage disease. *Am. J. Clin. Nutr.* *65*, 1507–1511.
4. Koeberl, D.D., Kishnani, P.S., Bali, D., and Chen, Y.T. (2009). Emerging therapies for glycogen storage disease type I. *Trends Endocrinol. Metab.* *20*, 252–258.
5. Kishnani, P.S., Austin, S.L., Abdenur, J.E., Arn, P., Bali, D.S., Boney, A., Chung, W.K., Dagli, A.I., Dale, D., Koeberl, D., et al.; American College of Medical Genetics and Genomics (2014). Diagnosis and management of glycogen storage disease type I: a practice guideline of the American College of Medical Genetics and Genomics. *Genet. Med.* *16*, e1.
6. Franco, L.M., Krishnamurthy, V., Bali, D., Weinstein, D.A., Arn, P., Clary, B., Boney, A., Sullivan, J., Frush, D.P., Chen, Y.T., and Kishnani, P.S. (2005). Hepatocellular carcinoma in glycogen storage disease type Ia: a case series. *J. Inher. Metab. Dis.* *28*, 153–162.
7. Reddy, S.K., Kishnani, P.S., Sullivan, J.A., Koeberl, D.D., Desai, D.M., Skinner, M.A., Rice, H.E., and Clary, B.M. (2007). Resection of hepatocellular adenoma in patients with glycogen storage disease type Ia. *J. Hepatol.* *47*, 658–663.
8. Margini, C., and Dufour, J.F. (2016). The story of HCC in NAFLD: from epidemiology, across pathogenesis, to prevention and treatment. *Liver Int.* *36*, 317–324.
9. Farah, B.L., Landau, D.J., Sinha, R.A., Brooks, E.D., Wu, Y., Fung, S.Y.S., Tanaka, T., Hirayama, M., Bay, B.H., Koeberl, D.D., and Yen, P.M. (2016). Induction of autophagy improves hepatic lipid metabolism in glucose-6-phosphatase deficiency. *J. Hepatol.* *64*, 370–379.
10. Klionsky, D.J., and Emr, S.D. (2000). Autophagy as a regulated pathway of cellular degradation. *Science* *290*, 1717–1721.

11. Waskowicz, L.R., Zhou, J., Landau, D.J., Brooks, E.D., Lim, A., Yavarow, Z.A., Kudo, T., Zhang, H., Wu, Y., Grant, S., et al. (2019). Bezafibrate induces autophagy and improves hepatic lipid metabolism in glycogen storage disease type Ia. *Hum. Mol. Genet.* 28, 143–154.
12. Takamura, A., Komatsu, M., Hara, T., Sakamoto, A., Kishi, C., Waguri, S., Eishi, Y., Hino, O., Tanaka, K., and Mizushima, N. (2011). Autophagy-deficient mice develop multiple liver tumors. *Genes Dev.* 25, 795–800.
13. Gjorgjieva, M., Calderaro, J., Monteillet, L., Silva, M., Raffin, M., Brevet, M., Romestaing, C., Roussel, D., Zucman-Rossi, J., Mithieux, G., and Rajas, F. (2018). Dietary exacerbation of metabolic stress leads to accelerated hepatic carcinogenesis in glycogen storage disease type Ia. *J. Hepatol.* 69, 1074–1087.
14. Koeberl, D.D., Sun, B.D., Damodaran, T.V., Brown, T., Millington, D.S., Benjamin, D.K., Jr., Bird, A., Schneider, A., Hillman, S., Jackson, M., et al. (2006). Early, sustained efficacy of adeno-associated virus vector-mediated gene therapy in glycogen storage disease type Ia. *Gene Ther.* 13, 1281–1289.
15. Koeberl, D.D., Pinto, C., Sun, B., Li, S., Kozink, D.M., Benjamin, D.K., Jr., Demaster, A.K., Kruse, M.A., Vaughn, V., Hillman, S., et al. (2008). AAV vector-mediated reversal of hypoglycemia in canine and murine glycogen storage disease type Ia. *Mol. Ther.* 16, 665–672.
16. Brooks, E.D., Landau, D.J., Everitt, J.I., Brown, T.T., Grady, K.M., Waskowicz, L., Bass, C.R., D'Angelo, J., Asfaw, Y.G., Williams, K., et al. (2018). Long-term complications of glycogen storage disease type Ia in the canine model treated with gene replacement therapy. *J. Inherit. Metab. Dis.* 41, 965–976.
17. Cunningham, S.C., Dane, A.P., Spinoulas, A., Logan, G.J., and Alexander, I.E. (2008). Gene delivery to the juvenile mouse liver using AAV2/8 vectors. *Mol. Ther.* 16, 1081–1088.
18. Weinstein, D.A., Correia, C.E., Conlon, T., Specht, A., Versteegen, J., Oncliv-Versteegen, K., Campbell-Thompson, M., Dhaliwal, G., Mirian, L., Cossette, H., et al. (2010). Adeno-associated virus-mediated correction of a canine model of glycogen storage disease type Ia. *Hum. Gene Ther.* 21, 903–910.
19. Yiu, W.H., Lee, Y.M., Peng, W.T., Pan, C.J., Mead, P.A., Mansfield, B.C., and Chou, J.Y. (2010). Complete normalization of hepatic G6PC deficiency in murine glycogen storage disease type Ia using gene therapy. *Mol. Ther.* 18, 1076–1084.
20. Lee, Y.M., Jun, H.S., Pan, C.J., Lin, S.R., Wilson, L.H., Mansfield, B.C., and Chou, J.Y. (2012). Prevention of hepatocellular adenoma and correction of metabolic abnormalities in murine glycogen storage disease type Ia by gene therapy. *Hepatology* 56, 1719–1729.
21. Luo, X., Hall, G., Li, S., Bird, A., Lavin, P.J., Winn, M.P., Kemper, A.R., Brown, T.T., and Koeberl, D.D. (2011). Hepatorenal correction in murine glycogen storage disease type I with a double-stranded adeno-associated virus vector. *Mol. Ther.* 19, 1961–1970.
22. Landau, D.J., Brooks, E.D., Perez-Pinera, P., Amarasekara, H., Mefferd, A., Li, S., Bird, A., Gersbach, C.A., and Koeberl, D.D. (2016). In Vivo Zinc Finger Nuclease-mediated Targeted Integration of a Glucose-6-phosphatase Transgene Promotes Survival in Mice With Glycogen Storage Disease Type IA. *Mol. Ther.* 24, 697–706.
23. Salganik, S.V., Weinstein, D.A., Shupe, T.D., Salganik, M., Pintilie, D.G., and Petersen, B.E. (2009). A detailed characterization of the adult mouse model of glycogen storage disease Ia. *Lab. Invest.* 89, 1032–1042.
24. Mutel, E., Abdul-Wahed, A., Ramamonjisoa, N., Stefanutti, A., Houberton, I., Cavassila, S., Pilleul, F., Beuf, O., Gautier-Stein, A., Penhoat, A., et al. (2011). Targeted deletion of liver glucose-6 phosphatase mimics glycogen storage disease type Ia including development of multiple adenomas. *J. Hepatol.* 54, 529–537.
25. Kishnani, P.S., Faulkner, E., VanCamp, S., Jackson, M., Brown, T., Boney, A., Koeberl, D., and Chen, Y.T. (2001). Canine model and genomic structural organization of glycogen storage disease type Ia (GSD Ia). *Vet. Pathol.* 38, 83–91.
26. Demaster, A., Luo, X., Curtis, S., Williams, K.D., Landau, D.J., Drake, E.J., Kozink, D.M., Bird, A., Crane, B., Sun, F., et al. (2012). Long-term efficacy following readministration of an adeno-associated virus vector in dogs with glycogen storage disease type Ia. *Hum. Gene Ther.* 23, 407–418.
27. Chandler, R.J., LaFave, M.C., Varshney, G.K., Trivedi, N.S., Carrillo-Carrasco, N., Senac, J.S., Wu, W., Hoffmann, V., Elkahoun, A.G., Burgess, S.M., and Venditti, C.P. (2015). Vector design influences hepatic genotoxicity after adeno-associated virus gene therapy. *J. Clin. Invest.* 125, 870–880.
28. Donsante, A., Miller, D.G., Li, Y., Vogler, C., Brunt, E.M., Russell, D.W., and Sands, M.S. (2007). AAV vector integration sites in mouse hepatocellular carcinoma. *Science* 317, 477.
29. Wang, P.R., Xu, M., Toffanin, S., Li, Y., Llovet, J.M., and Russell, D.W. (2012). Induction of hepatocellular carcinoma by in vivo gene targeting. *Proc. Natl. Acad. Sci. USA* 109, 11264–11269.
30. Donsante, A., Vogler, C., Muzyczka, N., Crawford, J.M., Barker, J., Flotte, T., Campbell-Thompson, M., Daly, T., and Sands, M.S. (2001). Observed incidence of tumorigenesis in long-term rodent studies of rAAV vectors. *Gene Ther.* 8, 1343–1346.
31. Kim, G.Y., Lee, Y.M., Kwon, J.H., Cho, J.H., Pan, C.J., Starost, M.F., Mansfield, B.C., and Chou, J.Y. (2017). Glycogen storage disease type Ia mice with less than 2% of normal hepatic glucose-6-phosphatase- $\alpha$  activity restored are at risk of developing hepatic tumors. *Mol. Genet. Metab.* 120, 229–234.
32. Cho, J.H., Kim, G.Y., Mansfield, B.C., and Chou, J.Y. (2018). Hepatic glucose-6-phosphatase- $\alpha$  deficiency leads to metabolic reprogramming in glycogen storage disease type Ia. *Biochem. Biophys. Res. Commun.* 498, 925–931.
33. Lee, Y.M., Conlon, T.J., Specht, A., Coleman, K.E., Brown, L.M., Estrella, A.M., Damska, M., Dahlberg, K.R., and Weinstein, D.A. (2018). Long-term safety and efficacy of AAV gene therapy in the canine model of glycogen storage disease type Ia. *J. Inherit. Metab. Dis.* 41, 977–984.
34. Brooks, E.D., Kishnani, P.S., and Koeberl, D.D. (2018). Letter to the Editors: Concerning “Long-term safety and efficacy of AAV gene therapy in the canine model of glycogen storage disease type Ia” by Lee et al. *J. Inherit. Metab. Dis.* 41, 913–914.
35. Bell, P., Moscioni, A.D., McCarter, R.J., Wu, D., Gao, G., Hoang, A., Sanmiguel, J.C., Sun, X., Wivel, N.A., Raper, S.E., et al. (2006). Analysis of tumors arising in male B6C3F1 mice with and without AAV vector delivery to liver. *Mol. Ther.* 14, 34–44.
36. Zhong, L., Malani, N., Li, M., Brady, T., Xie, J., Bell, P., Li, S., Jones, H., Wilson, J.M., Flotte, T.R., et al. (2013). Recombinant adeno-associated virus integration sites in murine liver after ornithine transcarbamylase gene correction. *Hum. Gene Ther.* 24, 520–525.
37. Chandler, R.J., LaFave, M.C., Varshney, G.K., Burgess, S.M., and Venditti, C.P. (2016). Genotoxicity in Mice Following AAV Gene Delivery: A Safety Concern for Human Gene Therapy? *Mol. Ther.* 24, 198–201.
38. Clar, J., Mutel, E., Gri, B., Creneguy, A., Stefanutti, A., Gaillard, S., Ferry, N., Beuf, O., Mithieux, G., Nguyen, T.H., and Rajas, F. (2015). Hepatic lentiviral gene transfer prevents the long-term onset of hepatic tumours of glycogen storage disease type Ia in mice. *Hum. Mol. Genet.* 24, 2287–2296.
39. Davidoff, A.M., Ng, C.Y., Zhou, J., Spence, Y., and Nathwani, A.C. (2003). Sex significantly influences transduction of murine liver by recombinant adeno-associated viral vectors through an androgen-dependent pathway. *Blood* 102, 480–488.
40. Sun, B., Zhang, H., Franco, L.M., Young, S.P., Schneider, A., Bird, A., Amalfitano, A., Chen, Y.T., and Koeberl, D.D. (2005). Efficacy of an adeno-associated virus 8-pseudotyped vector in glycogen storage disease type II. *Mol. Ther.* 11, 57–65.
41. Han, S.O., Ronzitti, G., Arnson, B., Leborgne, C., Li, S., Mingozzi, F., and Koeberl, D. (2017). Low-dose liver-targeted gene therapy for Pompe disease enhances therapeutic efficacy of ert via immune tolerance induction. *Mol. Ther. Methods Clin. Dev.* 4, 126–136.
42. Mural, R.J., Adams, M.D., Myers, E.W., Smith, H.O., Miklos, G.L., Wides, R., Halpern, A., Li, P.W., Sutton, G.G., Nadeau, J., et al. (2002). A comparison of whole-genome shotgun-derived mouse chromosome 16 and the human genome. *Science* 296, 1661–1671.
43. Perez-Pinera, P., Ousterout, D.G., Brown, M.T., and Gersbach, C.A. (2012). Gene targeting to the ROSA26 locus directed by engineered zinc finger nucleases. *Nucleic Acids Res.* 40, 3741–3752.
44. Hirt, B. (1967). Selective extraction of polyoma DNA from infected mouse cell cultures. *J. Mol. Biol.* 26, 365–369.
45. Livak, K.J., and Schmittgen, T.D. (2001). Analysis of relative gene expression data using real-time quantitative PCR and the 2<sup>-</sup>(Delta Delta C(T)) Method. *Methods* 25, 402–408.